Journal of Applied Polymer Science

Hydrophobic Microblock Length Effect on the Interaction Strength and Binding Capacity Between a Partially Hydrolyzed Microblock Hydrophobically Associating Polyacrylamide Terpolymer and Surfactant

Yongjun Guo,[1,2,3] Yan Liang,[1,2] Xueshan Yang,[3] Rusen Feng,[1,2] Rutong Song,[1,2] Jingda Zhou,[1,2] Feilong Gao[1,2]

[1]State Key Laboratory of Oil and Gas Reservoir Geology and Exploitation, Southwest Petroleum University, Chengdu 610500, People's Republic of China

[2]School of Chemistry and Chemical Engineering, Southwest Petroleum University, Chengdu 610500, People's Republic of China

[3]Sichuan Guangya Polymer Chemical Company, Limited, Nanchong 637500, People's Republic of China

Correspondence to: Y. Guo (E-mail: gyfzgyj@126.com)

ABSTRACT: Poly(acrylamide/sodium acrylate/*N*-dodecyl acrylamide)s [poly(AM/NaAA/C_{12}AM)s] with different hydrophobic microblock lengths (N_H's) were prepared by the micellar copolymerization of acrylamide and sodium acrylate with a low amount of *N*-dodecyl acrylamide (0.2 mol %), and the molecular structure was characterized by Fourier transform infrared spectroscopy, ^{1}H-NMR, and static light scattering. A combination of experiments involving viscosity measurement, fluorescence, and conductometry was applied to investigate the effect of N_H on the interaction strength and binding capacity between poly(AM/NaAA/C_{12}AM)s and $C_{12}H_{25}SO_4Na$ [sodium dodecyl sulfate (SDS)]. The viscosity, I_3/I_1 (the intensity ratio of the third vibrational band to the first band of pyrene molecules), and conductivity of the mixed system of copolymers with SDS all had different variation trends with the concentration of SDS. The binding capacity of the copolymers with SDS was calculated according to quantitative differences between the critical micelle concentration of the pure SDS solution and the mixed system. All of the results show that the interaction strength of SDS with the copolymers rose, and the binding capacity decreased with increasing N_H. © 2014 Wiley Periodicals, Inc. J. Appl. Polym. Sci. **2014**, *131*, 40633.

KEYWORDS: copolymers; electrochemistry; spectroscopy; surfactants; viscosity and viscoelasticity

Received 22 November 2013; accepted 21 February 2014

DOI: 10.1002/app.40633

INTRODUCTION

Over the past few decades, partially hydrolyzed polyacrylamide (HPAM) has been widely applied in chemical flooding technologies for enhanced oil recovery (EOR) because of its better resistance to biodegradation and its ability to enhance viscosity compared to biopolymers.[1–6] The viscosity of the HPAM solution increases with its increasing molecular weight. However, the HPAM solution shows a tremendous viscosity loss and is extremely sensitive to the physicochemical conditions (shear rate, ion content, temperature, pH, etc.) in the field application.[7–11] So, HPAM has great limitations, and other polymers that provide excellent properties must be developed to meet application requirements.

Nowadays, water-soluble hydrophobically associating polyacrylamides (HAPAMs) with a small number of hydrophobic groups have attracted extensive attention in both academic and industrial laboratories, and they have been investigated as a possible substitute for HPAM polymers in EOR applications.[11–23] Because the hydrophobic interactions and association of hydrophobic groups can build a reversible transitory three-dimensional network structure,[6,9,24,25] these polymers can effectively increase the hydrodynamic volume of the polymer chain in solution. Therefore, HAPAMs own many unique properties compared with conventional HPAM; these include a significant viscosity enhancement,[26–28] time-dependent effects,[26,29] a marked viscoelasticity,[30,31] shear thinning and thickening,[32] and excellent shearing/temperature/salinity stability.[12,33] In addition, HAPAMs can interact with small-molecule surfactants[34–36] through the hydrophobic chains along the molecular skeleton to form polymer/surfactant binary systems owning special microstructures and rheological properties in aqueous solutions.[37–40] In these cases, HAPAMs convey a huge potential for EOR applications. At present, some HAPAMs have been successfully applied for mobility control in EOR.[41,42] However, the solubility of HAPAMs is an important consideration in oilfield applications because the poor solubility will impact the injectivity and lead to formation damage. The solubility can be improved

© 2014 Wiley Periodicals, Inc.

through the introduction of hydrolyzing amide groups (e.g., sodium acrylic acid) or sulfonate-containing monomers to increase the ionic character.[10,12]

In general, HAPAMs can be classified into two main classes: one is the telechelic type, in which the linear chains are normally end-capped with hydrophobic groups;[43,44] the other is the multisticker type, which is composed of one or more hydrophobic monomer molecules forming tiny segments and distributing as isolated units or small blocks on the polymer main chains.[19,44–46] The rheological properties of both types have marked differences that are affected by the structural characteristics (the content, nature, and distribution of hydrophobes; block length; molecular weight; etc.).[19,47] Partially hydrolyzed microblock hydrophobically associating polyacrylamides (HMBHAPs) are typic multisticker associating polymers. The synergistic or noncollaborative interaction between HMBHAPs and surfactants can cause much variation in the structural performance, viscosity, and so on.[48] Some surfactants, whose concentrations are appropriate, are favorable for polymer/surfactant systems in many aspects, such as increasing the viscosity[49,50] and improving the rheological behaviors.[50,51] On the other hand, other surfactants and the lower or higher concentration of surfactant all have adverse effects on the system performances and cause, for instance, poor viscoelasticity[51] and unstable solution properties. As for the HMBHAP/surfactant system, a hydrophobic microblock length (N_H) is often required to obtain a best match and design to guarantee good solution properties. For the aforementioned reasons, the study of the effects of N_H on the interaction strength and binding capacity between surfactants and HMBHAPs has a very important significance in the effective regulation of the performance of polymer/surfactant systems and for providing a favorable theoretical basis for practical applications through the enhancement of the positive synergetic effects and the reduction of negative impacts.

There have been a wide variety of studies on the binding interaction of surfactants with nonassociating polymers or telechelic associating polymers in the past few decades, and excellent review articles are available that describe the interactions between nonionic and ionic surfactants with polymers.[52–65] Many physicochemical techniques involving fluorescence,[65,66] electromotive force, potentiometry,[58,60,61,67] isothermal titration microcalorimetry,[58,60,61,63] differential scanning calorimetry, light scattering,[68] conductometry,[63] surface tension,[9,69,70] dialysis,[34] rheological measurement,[40,71] turbidity and NMR self-diffusion,[63,72] and small-angle neutron scattering[34,61,69,72] have been involved in these studies. The interaction mechanisms of polymers and surfactants have been given and discussed. For example, Bystryak,[52] Sovilj,[73] and Wang et al.[63] investigated the poly(ethylene imine)/sodium dodecyl sulfate (SDS), the hydroxypropyl methyl cellulose/SDS (HPMC/SDS), and the branched poly(ethylene imine)/SDS systems, respectively, by conductometry. They obtained similar results; that is, there was an initial linear increase in conductivity with increasing SDS concentration, and two break points gradually appeared. Then, an evident decrease existed in the slope between the two points, and there was the same slope as for SDS without the polymer above the second point. The consequences were explained by the depletion of free ions of the surfactant from solution or cluster formation with the polymer on account of binding interactions. When all of the binding sites on the polymer were saturated with SDS molecules, the free micelles of surfactants began to form.

However, so far there have been no reports on the variation of interaction strengths between HMBHAPs and surfactants from the perspective of the binding capacity as studied by conductometry,[23,40] and the study of the effect of N_H on the interaction and binding capacity has not been carried out. In this study, we synthesized different microblock terpolymers of acrylamide (AM), sodium acrylate (NaAA), and *N*-dodecyl acrylamide (C_{12}AM) by micellar polymerization and investigated the effects of N_H on the interaction strength and binding capacity of the terpolymers with SDS by combination experiments of viscosity measurement, fluorescence, and conductometry. The results show that the interaction strength was enhanced and the binding capacity decreased with increasing N_H.

EXPERIMENTAL

Materials

AM was purchased from Jiangxi Changjiu Biological and Chemical Corp. (China). The synthesis and purification of C_{12}AM were described elsewhere.[74] NaAA was made by the mixture of sodium hydroxide with filtered acrylic acid at a certain molar ratio (1:1) and the repeated filtration of the reaction solution. SDS ($C_{12}H_{25}SO_4Na$; Chengdu Kelong, China, 98%) was double-recrystallized from ethanol. Pyrene (Acros Organics, 98%) was recrystallized from ethanol and sublimed twice. Ultrapure water was made in an ultrapure water purification system. Microblock hydrophobically associating poly(acrylamide/sodium acrylate/*N*-dodecyl acrylamide)s [poly(AM/NaAA/C_{12}AM)s] was initiated to polymerize by 2,2′-azobis(2-methyl propionamide) dihydrochloride. The specific methods of synthesis and purification are given later. AM and 2,2′-azobis(2-methyl propionamide) dihydrochloride were used without further purification.

Polymerization

In the previous 2 decades, the Francoise Candau research group (France, CRM) achieved a leading position in the synthesis of multisticker polymers by micellar polymerization. Candau, Selb, and coworkers[75–85] showed that in the micellar polymerization process, hydrophobic monomers solubilized within surfactant micelles, whereas hydrophilic monomers were dissolved in the aqueous continuous medium. Because of the high local concentration in the micelles, hydrophobic monomers were randomly distributed as small blocks in the hydrophilic backbone. Moreover, Candau and coworkers[78,82] assumed that the length of hydrophobic blocks corresponded roughly to the number of hydrophobes per micelle (N_H). Therefore, in this case, N_H was calculated from eq. (1):[82,86]

$$N_H = \frac{C_{HM}}{(C_s - \mathrm{cmc})/N_{\mathrm{agg}}} \quad (1)$$

where C_{HM} is the molar concentration of the hydrophobic monomer, C_s is the molar concentration of the surfactant, cmc is the critical micelle concentration of the surfactant, N_{agg} is the micellar aggregation number of the surfactant. Because the surfactant concentration is always well above the cmc in the

Table I. Polymerization and Structural Parameters of the HMBHAPs

		Polymerization parameter				Structural parameter		
Sample	N_H[a]	AM (g; 41.5 wt %)	NaAA (g; 28.66 wt %)	C_{12}AM (g; 100 wt %)	SDS (g; 100 wt %)[b]	$[\eta]$ (mL/g)	M_η ($\times 10^6$)	M_w ($\times 10^6$)
N_1	1.02	49.84	31.85	0.19	14.88	1520.75	7.62	5.91
N_2	2.49	49.84	31.85	0.19	5.81	1179.55	5.54	3.93
N_3	3.72	49.84	31.85	0.19	4.02	1023.51	4.64	3.29

$[\eta]$, intrinsic viscosity; M_η, viscosity-average molecular weight.
[a] With an aggregation number of 60 and a cmc value of 9.2×10^{-3} mol/L for SDS at 50°C.
[b] The cmc values for SDS were 5.6, 2.2, and 1.5.

micellar polymerization, when the cmc is ignored, eq. (1) can be approximately equal to eq. (2):

$$N_H \approx \frac{C_{HM}}{C_s} \times N_{agg} = \frac{N_{agg}}{SMR} \quad (2)$$

where SMR is the molar ratio of surfactant to hydrophobic monomer. In this article, microblock hydrophobically associating poly(AM/NaAA/C_{12}AM)s were prepared by the aqueous micellar copolymerization of AM, sodium acrylate, and a small fraction (0.2 mol %) of C_{12}AM (the polymerization parameters are shown in Table I), where the SMR value was changed to adjust N_H.[6,37,76,87,88]

The calculated amounts of AM, NaAA, SDS, ultrapure water, and hydrophobic monomer (C_{12}AM) were added to the beaker; the mixture was homogenized by stirring and degassed for 30 min with nitrogen at 50°C. Then, 3 mL of water-soluble 2,2′-azobis(2-methyl propionamide) dihydrochloride (1 wt %) was added as an initiator, and nitrogen was continually bubbled for 10 min. After 2 h, the reaction was terminated by the removal of the copolymer gels and cooling to room temperature. The products were washed and precipitated repeatedly in ethanol before they were vacuum-dried for 24 h at 50°C to eliminate residual moisture. As a result, poly(AM/NaAA/C_{12}AM)s with increasing N_H were obtained and were abbreviated as N_1, N_2, and N_3 (they are collectively referred to as the HMBHAPs); their molecular structures and structural parameters are shown in Figure 1 and Table I. The total monomer concentration was 20 wt %, and the content of hydrophobic monomers was 0.2 mol %. All of the copolymer samples examined here were prepared during a single copolymerization reaction.

Characterization

The HMBHAPs were characterized by Fourier transform infrared (FTIR) spectroscopy, ^{1}H-NMR, and static light scattering.

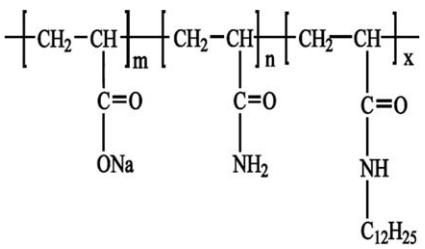

Figure 1. Molecular structure of the HMBHAPs.

The results confirm the existence of the hydrophobic monomer in the copolymers. FTIR (Figure 2) measurements were performed on a Nicolet 6700 FTIR spectrometer (Thermo Fisher) with the KBr tablet method. ^{1}H-NMR (Figure 3) experiments (400 MHz) were conducted on a Bruker AV-III NMR spectrometer (Bruker BioSpin, Switzerland), and chemical shifts in D_2O are quoted as δ values in parts per million and the coupling constants are listed in hertz. The following abbreviations are used to indicate the magnitude or multiplicity: w = weak, m = moderate or multiplet, s = strong or singlet, d = doublet, and t = triplet. The Zimm plots (Figure 4) were obtained from a BI-200SM laser light scatterometer (Brookhaven) equipped with a 515 chromatograph, BI-MWA multi-angle laser light scatterometer, BI-DNDC differential refractometer, and analog thermostat. Finally, the value of the weight-average molecular weight (M_w) is listed in Table I.

IR (cm^{-1}, KBr, ν): 3580 [s; ν_{as}(N—H)], 3182 [s, ν_s(N—H)], 2929 [m, ν_{as}(C—H)], 1680 [s, ν_s(C═O)], 1560 (s), 1413 [m, ν_s(C—N)], 1327 (w), 1119 (w). ^{1}H-NMR (400 MHz, D_2O, δ): 4.66 (s, 2H, D_2O), 3.49–3.50 (d, J = 8 Hz, 2H, —CH_2NHR), 2.39 (m, 1H, —CH), 2.07 (s, 1H, —CHCOR), 1.49 (d, J = 7.5 Hz, 2H, —CH_2), 1.01–1.04 (t, J = 7 Hz, 3H, —CH_3). J is the coupling constant.

The measurement conditions and pretreatment of the Zimm plots of the HMBHAPs from static light scattering: solvent,

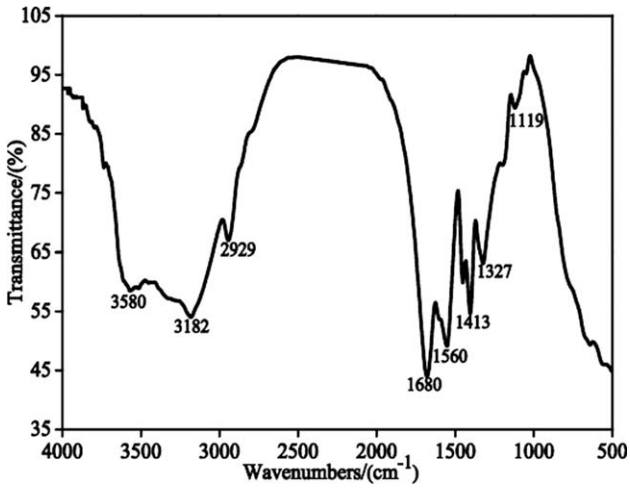

Figure 2. FTIR spectrum of the HMBHAPs.

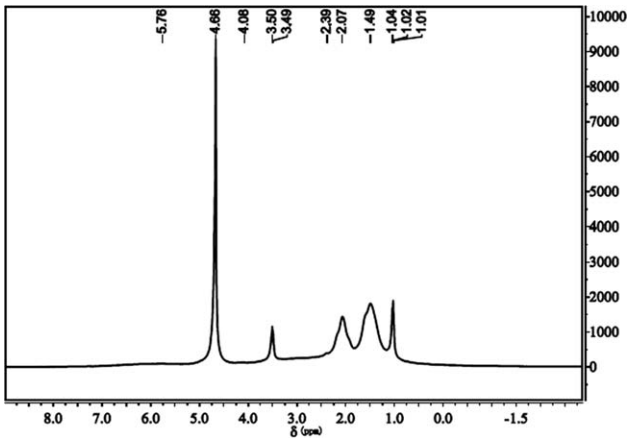

Figure 3. ^{1}H-NMR spectrum of the HMBHAPs.

formamide, and pure water (volume ratio = 1:1) in 1 mol/L NaCl solution (the refractive index increment dn/dc = 0.161 mL/g), and the solution was filtered with a 0.25-μm membrane to dust before the test.

Generally speaking, if a hydrophobe bears a chromophores such as phenyl or other aromatic groups, the hydrophobe content of a copolymer can be determined accurately by UV spectroscopy.[78,79,81] ^{1}H-NMR is also generally accurate for determining the hydrophobe content if the hydrophobic level is above 1 mol % or the hydrophobe contains two terminal methyl groups as *N,N*-dihexyl acrylamide.[76,78,79] However, in our case, the hydrophobic monomer consists of alkyl chains; no accurate results could be obtained by these methods because the extremely low amount of hydrophobes (0.2 mol %). As a result, we implicitly assumed that the actual level was equivalent to the initial feed content as some authors mentioned.[78,79,89] In addition, there was no significant difference among the M_w values of the HMBHAPs (shown in Table I), so a meaningful comparison of their solution properties was made, as shown later.

Solution Preparation

1. Dry powder of the HMBHAPs were mixed with ultrapure water with stirring to make a 5000 mg/L mother liquor, and this was left still for more than 24 h before use.
2. The stoichiometric SDS was predried for 3 h at 80°C, weighed accurately, and added to a 500-mL flask with 400 mL of ultrapure water. The flask was placed in an ultrasonic cleaner to oscillate for 5 min. Then, the stock solution (5×10^{-2} mol/L) was obtained by the addition of water to the mark line.
3. At a fixed HMBHAP concentration, as a function of the SDS concentration, the copolymer mother liquor (5000 mg/L) and the SDS solution (5×10^{-2} mol/L) were diluted and made up of the mixed solutions of HMBHAPs (3000, 3500, and 4500 mg/L) and SDS (a series of concentration).
4. With ethanol as the solvent, 0.0202 g of pyrene was weighed precisely and added to a 100-mL flask. Then, we made a solution in which pyrene concentration was 1×10^{-3} mol/L by marking the line. Furthermore, the solution was diluted to 1×10^{-4} mol/L as a reserve.
5. With a pipette, 0.6 mL of a pyrene solution (1×10^{-4} mol/L) was placed in a beaker and diluted to 30 mL with the previous mixed solutions (prepared in step 3) after the ethanol

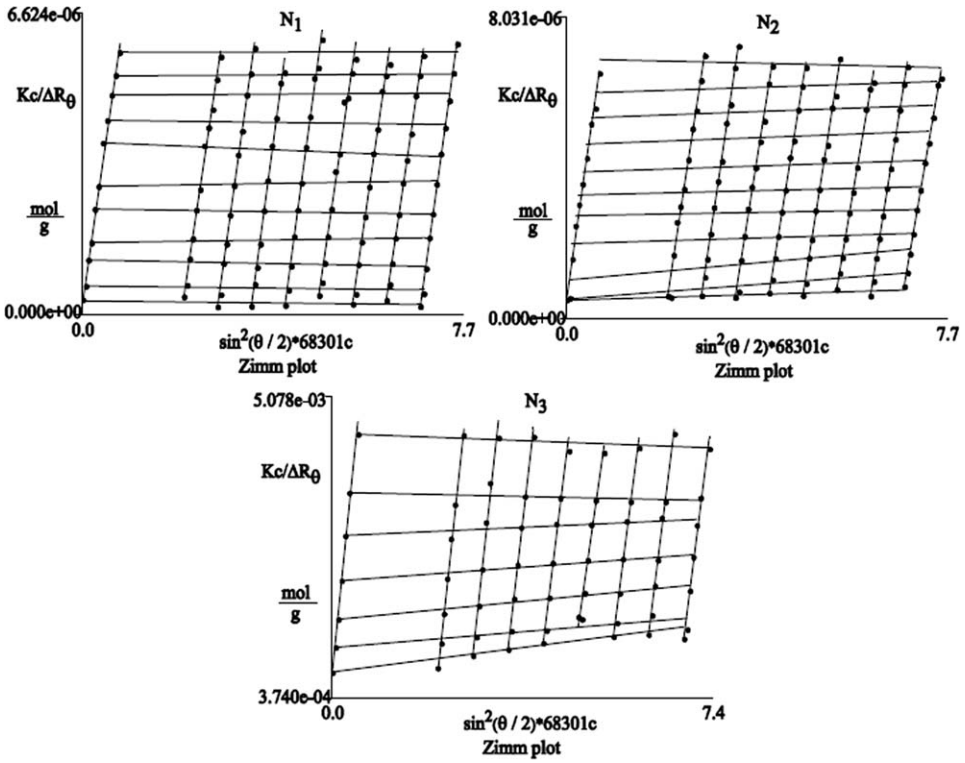

Figure 4. Zimm plots of the HMBHAPs from static light scattering: K, optical constant; c, solution concentration; θ, scattering angle; R_θ, Rayleigh ratio.

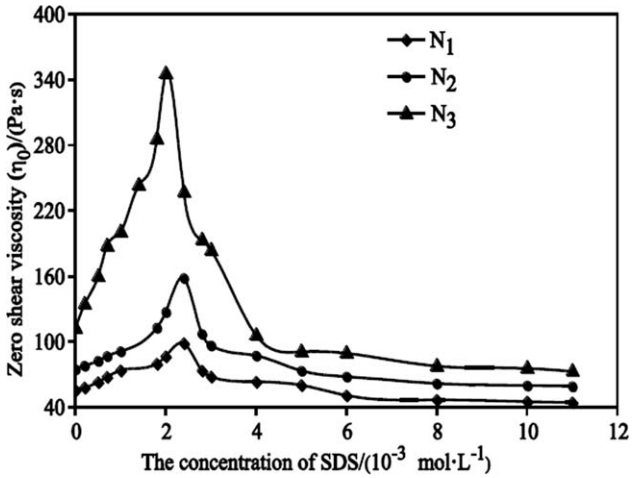

Figure 5. Variation of the zero-shear viscosity as a function of the concentration of SDS for the HMBHAP/SDS mixed systems at a concentration of 3000 mg/L.

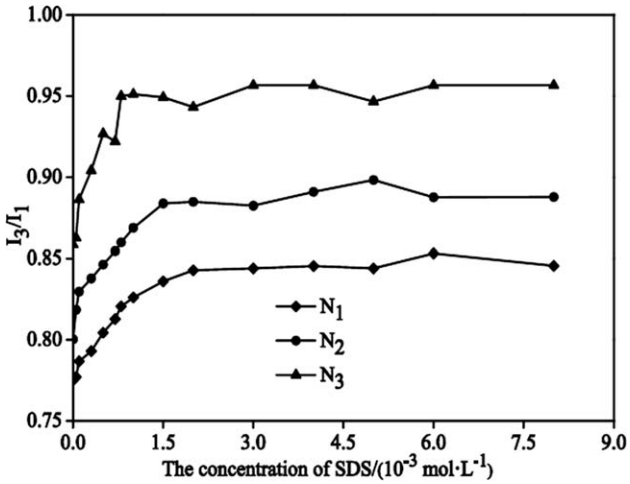

Figure 6. Variation of I_3/I_1 as a function of the concentration of SDS for the pyrene-labeled HMBHAP/SDS mixed systems at a concentration of 3000 mg/L.

completely volatilized. Thus, HMBHAP/SDS mixed solutions labeled by pyrene (concentration = 2×10^{-6} mol/L) were obtained.

6. Before the measurements, all samples were mixed by a magnetic stirrer and left still for at least 2 h.

Viscosity Measurement

The stress–sweep viscosity curves of the HMBHAP/SDS mixed system were obtain on a physical MCR301 rheometer (Anton Paar) with the functionality of an automatic data record and storage at 30°C. The measuring system was the cone-and-plate geometry system (CP75-1, 2° angle, and 75-mm diameter), and the stress was 0.001–10 Pa. The zero-shear viscosity (η_0) was calculated according to the Carreau–Yasuda rheological model [eq. (3)], and the variation plots of η_0 versus the SDS concentration were made from the data:[90]

$$y=(y_0-y_{\inf}) * [1+(\lambda * x)^a]^{\frac{n-1}{a}}+y_{\inf} \quad (3)$$

where y is the viscosity input data, x is the shear rate input data, λ is the characteristic relaxation time, a is the Carreau constant, n is the Carreau index, y_0 is the zero-shear viscosity, $y_{\inf}$ is the infinite shear viscosity, and y_0 is always greater than $y_{\inf}$.

Table II. Tackifying Amplitudes and Intervals of the Different HMBHAP/SDS Mixed Systems

Sample	Initial viscosity (Pa s)	Maximum viscosity (Pa s)	Tackifing amplitude (%)[a]	Tackifing interval (10^{-3} mol/L)[b]
N_1	55.80	98.75	176.97	0-6
N_2	75.02	158.43	211.18	0-5
N_3	112.51	345.51	307.09	0-4

[a] Percentage of the maximum viscosity and initial viscosity.
[b] SDS concentration range in which the viscosity is always higher than the initial viscosity.

Fluorescence Study

The fluorescence spectra were recorded on a Cary Eclipse fluorescence spectrophotometer with a Czemy–Tumer monochromator (resolution = 1.5 nm, accuracy = 1 nm). The excitation wavelength was 335 nm, and the excitation/emission slit was 5 nm in all of the experiments. Pyrene-labeled HMBHAP/SDS mixed solutions were added to 1-cm quartz cells for the measurements. The emission and excitation spectra of the solutions were recorded with front-face detection. The emission spectra were not corrected.

Conductivity Determination

The conductivities of the SDS solution and the mixed system of HMBHAPs with SDS were determined on a DDS-307A conductivity meter equipped with a platinized platinum electrode at 30°C. Curves of the specific conductance alternated with the SDS concentration were also plotted from the data.

RESULTS AND DISCUSSION

Zero-Shear Viscosity Analysis

As shown in Figure 5, the zero-shear viscosity of the mixed systems of the copolymers with SDS passed through a maximum with increasing SDS concentration (SDS concentration $\approx 2 \times 10^{-3}$ mol/L) and reached a minimum where the concentration of SDS was around 8×10^{-3} mol/L (cmc of SDS). These effects were ascribed to the result of two opposing processes: one was the formation of mixed micellar-like aggregates containing alkyl chains belonging to the surfactant molecules and copolymers by crosslinking and bridging patterns, and the other was the replacement and collapse for micellar-type aggregates by unifunctional aggregates and pure surfactant micelles.[38,39,48,50,91–97]

However, what we must emphasize is that the increasing rates of viscosity were enhanced slowly at first and then showed a steep increase before the maximum viscosity point. This result was correlated with two issues: one was the number of mixed micellar aggregates, and another was their lifetimes. It is well known that the hydrophobic groups of copolymer chains can associate to form intramolecular and intermolecular crosslinks.

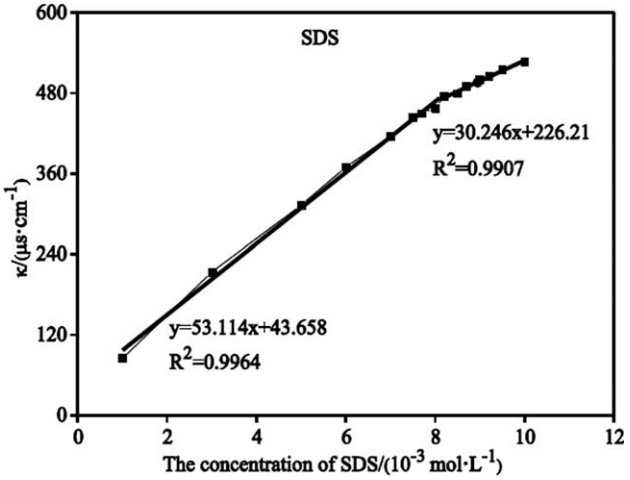

Figure 7. Conductivity versus concentration in the SDS solutions.

When SDS was mixed with HMBHAPs, the hydrophobic units extended into the crosslinks to make the many hydrophobic groups of HMBHAPs exposed. Thus, some associations changed from intramolecular to intermolecular association or many intermolecular mixed micellar junctions whose lifetimes were stronger began to form or the number of junctions increased. Piculell et al.[40] found that the lifetimes of the mixed micellar junctions formed by hydrophobically modified hydroxyethyl cellulose (HMHEC) with nine anionic and cationic surfactants (excluding SDS) increased across the viscosity maximum, whereas the number of mixed micellar junctions decreased. However, this conclusion is not necessarily applicable to the HMBHAP/SDS system. To that end, the factor that played a dominant role needs to be further studied with other feasible methods, such as rheological measurement[40,44,50,98] and fluorescence study.[99,100]

In addition, as shown in Figure 5 and Table II, the increasing rates and amplitudes of viscosity increase with increasing N_H; on the contrary, the tackifying intervals decrease. These phenomena can be interpreted to mean that HMBHAPs with longer N_H's have more hydrophobic moieties on each hydrophobic microblock of the copolymer molecular chains so that there are more intermolecular association structures instead of intramolecular associations. With the addition of SDS, the strength (i.e., lifetime) or the number of intermolecular association structures increases pronouncedly. However, what the main factor is still needs to be clarified. Furthermore, the rule of viscosity changing with the concentration of SDS at the HMBHAP concentration of 3500 or 4500 mg/L was same as 3000 mg/L, so the plots are not given, and this is discussed further.

Fluorescence Analysis

From the pyrene emission spectra, an intensity ratio was calculated: the intensity ratio of the third vibrational band (at 383.5 nm) to the first band (at 373 nm; I_3/I_1).[65,101] There was a consistent law of I_3/I_1 changing with the concentration of SDS in pyrene-labeled HMBHAP/SDS mixed solutions (shown in Figure 6). Above all, I_3/I_1 steeply increased with the concentration of

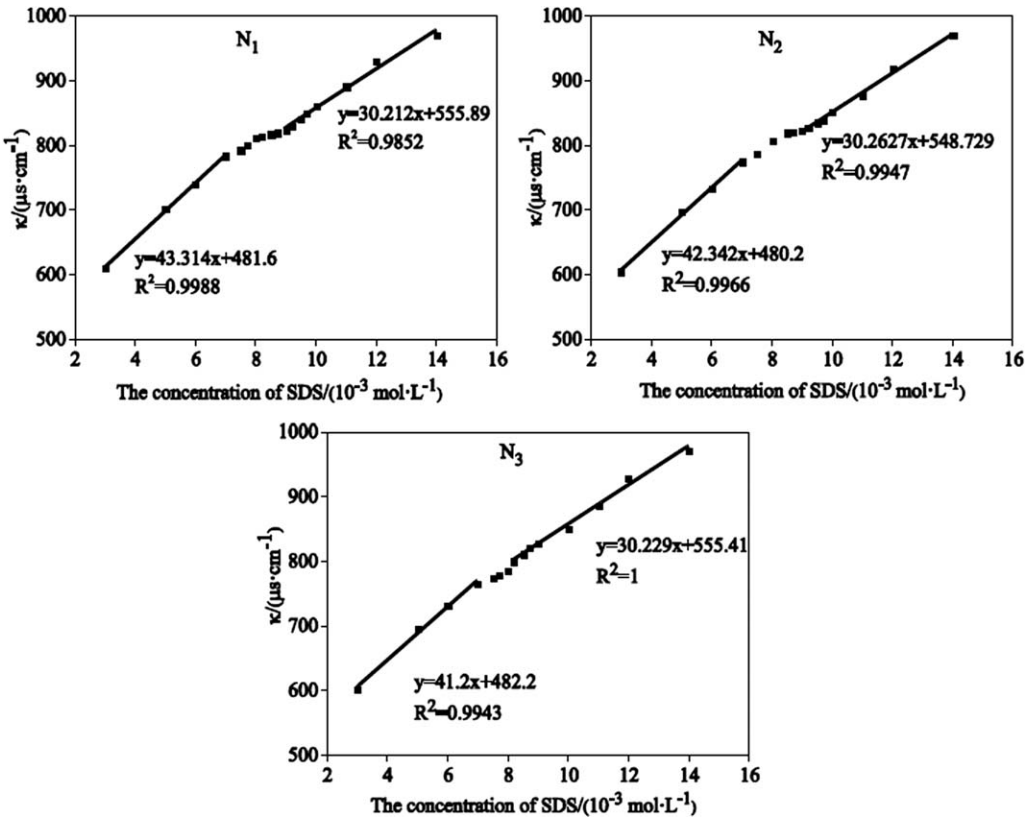

Figure 8. Variation of the conductivity as a function of the concentration of SDS for the HMBHAP/SDS mixed solutions at a concentration of 3000 mg/L.

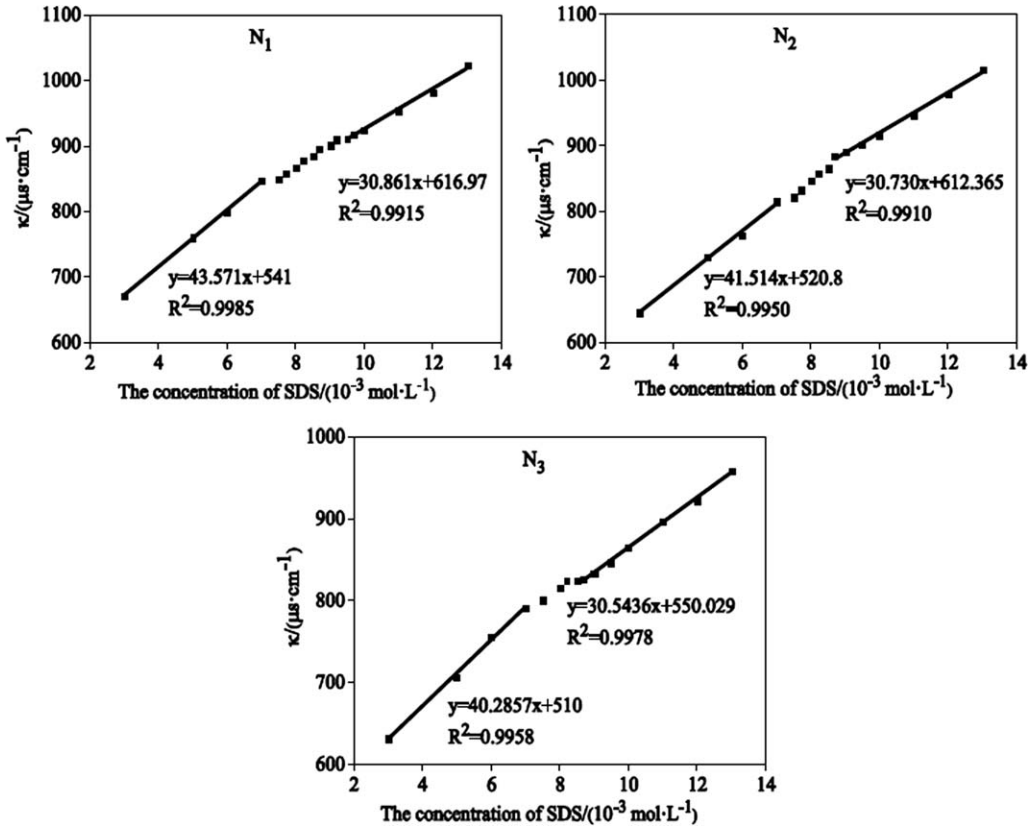

Figure 9. Variation of the conductivity as a function of the concentration of SDS for the HMBHAP/SDS mixed solutions at a concentration of 3500 mg/L.

SDS, then increased at a relatively slow rate, and ultimately reached a plateau above a certain concentration. In addition, with increasing N_H, I_3/I_1 increased, and the plateau occurred at a lower concentration of SDS. The concentrations of SDS corresponding to the break points of the plateaus, respectively, were 2×10^{-3} mg/L (N_1), 1.5×10^{-3} mg/L (N_2), and 1×10^{-3} mg/L (N_3).

These results could be interpreted such that in the presence of SDS in solutions, SDS could interact with HMBHAPs to form mixed micellelike aggregates, where there were many hydrophobic microdomains enriched by SDS molecules. As a result, the compactness of the hydrophobic domains increased, and the average micropolarity of the solution decreased; this enable more pyrene molecules to solubilize in hydrophobic domains and caused I_3/I_1 to increase.[99,100,102,103] The structure of the hydrophobic domains was basically stable at a certain concentration of SDS so that I_3/I_1 reached a stable value. This interpretation suggests that the interaction strength of the HMBHAPs with SDS gradually increased with the SDS concentration before it reached stability.

Although the inconsistent increase of I_3/I_1 before the stable value was related to the different increase degrees (caused by the SDS molecules) for the compactness of hydrophobic domains, when SDS was mixed with HMBHAPs initially, a certain number of SDS molecules interacted with the HMBHAPs to cause an obvious enhancement in the lifetime of mixed micellelike aggregates in a certain concentration range of SDS, whereas more SDS molecules only caused a slow increase in the lifetime outside the range. Meanwhile, when the N_H was longer, the I_3/I_1 was greater, and the SDS concentration corresponding to the platform was lower; this indicated that the tightness of the hydrophobic domains was larger, and the number of SDS molecules needed to form a steady structure was lower with rising N_H. Undoubtedly, this also showed that the interaction strength between the HMBHAPs and SDS increased with N_H; this demonstrated that the increase in the lifetime was one of main factors in the previous results obtained from the viscosity measurements. The same trends were seen for the other mixed systems, where the concentrations of HMBHAPs were 3500 or 4500 mg/L, and the results are not discussed further in detail.

Conductivity Analysis

Specific conductance is a parameter representing the conductive performance of materials, such as metals, semiconductors, and electrolyte solutions. When the conductivity is greater, the conductive performance is stronger. The temperature, doping level, and anisotropy are the main factors affecting conductivity. For electrolyte solutions, the conductivity (κ) can be calculated on the basis of eq. (4).

$$\kappa = G\frac{l}{A} = G \cdot K \tag{4}$$

where G is the conductance, l is the conductive length, A is the conducting cross-sectional area, and K is the electrode constant. Because K is a constant for a fixed electrode, κ is only related to G, whereas G depends on the solution concentration, the dissociation coefficient, and the migration rate of ionic in

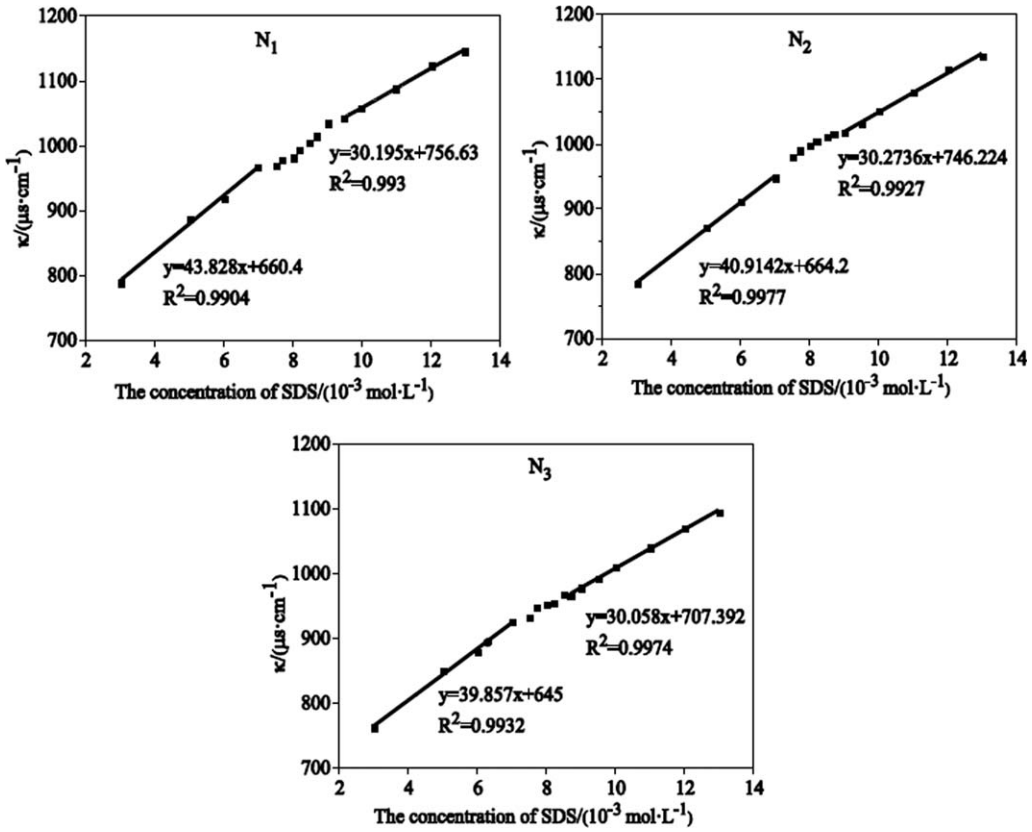

Figure 10. Variation of the conductivity as a function of the concentration of SDS for the HMBHAP/SDS mixed solutions at a concentration of 4500 mg/L.

solution.[104] Therefore, when the temperature and other external conditions were invariable, κ also relies on these three factors.

cmc is the lowest concentration at which surfactant molecules aggregate to form free micelles in solution.[105–107] It is an important feature of surfactants: as the cmc decreases, the concentration required to make the micelles free and to reach saturated surface (interfacial) adsorption decreases. In the presence of HMBHAPs, the SDS molecules liaisoned with hydrophobe units to constitute a hydrophobic domain where SDS was incorporated; this resulted in the variation of the cmc of SDS in the mixed system. Therefore, the method, the measurement of the cmc of SDS in pure and mixed solutions, respectively, could be used to investigate the effect of N_H on the interaction strength and binding capacity between HMBHAPs and SDS.

SDS cmc

The curve of conductivity alternating with the concentration in SDS solutions was plotted from the data. A significant inflection point occurred, so the piecewise linear fit was made on the curve (shown in Figure 7).

According to Figure 7, the slopes of the fitting curve before and after the turning point could be denoted, respectively, as k_1 and k_2.

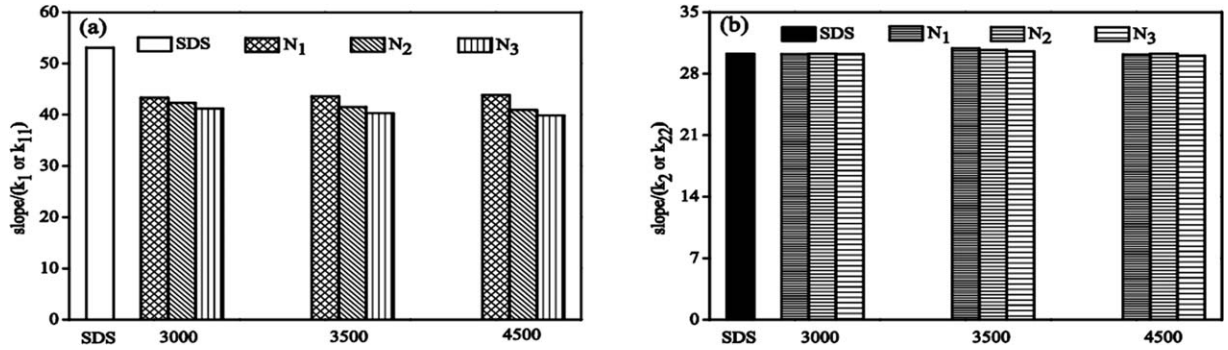

Figure 11. Segment-fitting slopes k_{11} and k_{22} for the conductivity curves of the HMBHAP/SDS system with different copolymer concentrations (3000, 3500, and 4500 mg/L) as a function of the SDS concentration: (a) k_1 (white column) and k_{11} (other columns) and (b) k_2 (black column) and k_{22} (other columns).

Table III. Binding Results for SDS with the HMBHAPs

Sample	Copolymer concentration (mg/L)	SDS cmc (10^{-3} mol/L)	C_1 (10^{-3} mol/L)	SDS cmc in the mixed system: C_2 (10^{-3} mol/L)	Binding concentration (10^{-3} mol/L)	Molar ratio (SDS/hydrophobes)
N_1	3000	7.98	7.00	9.00	1.02	13.10:1
N_2	3000	7.98	7.00	8.50	0.52	6.67:1
N_3	3000	7.98	7.00	8.20	0.22	2.81:1
N_1	3500	7.98	7.00	9.20	1.23	13.51:1
N_2	3500	7.98	7.00	8.70	0.72	7.92:1
N_3	3500	7.98	7.00	8.50	0.52	5.71:1
N_1	4500	7.98	7.00	9.50	1.53	13.09:1
N_2	4500	7.98	7.00	9.00	1.02	8.74:1
N_3	4500	7.98	7.00	8.70	0.72	6.16:1

k_1 was greater than k_2; this illustrated that the variation amplitude of the conductivity was inconsistent as a function of increasing concentration in the SDS solutions. That is, the dissociation coefficient and the ionic migration rate were greater before the point. This result was related to the reaching of the cmc of SDS at the break point at which the SDS molecules formed free micelles to reduce the dissociation degree of SDS. Consequently, the concentration (7.98×10^{-3} mol/L) corresponding to the inflexion was the cmc of SDS at room temperature. This cmc was consistent with the values reported (8.00×10^{-3} and 8.08×10^{-3} mol/L) in the literature by conductivity.[39,108]

Binding Interaction of HMBHAPs with SDS

As shown in Figures 8–10, there was very good agreement on the conductivity conversion with the concentration of SDS in the HMBHAP/SDS mixed solutions at room temperature. Two break points, namely, C_1 and C_2, existed on the curve. Thereby, the curve was made into a linear segment fit to obtain the differential slopes, which were denoted as k_{11} and k_{22}. The conductivity increased linearly with the concentration of SDS below C_1 and above C_2, and k_{11} was greater than k_{22}. However, the conductivity aggrandized nonlinearly between C_1 and C_2, and the amplitude decreased and even leveled off. It was apparent that the dissociation coefficient and the migration rate of ions in the mixed solutions were different at each various stage.

In addition, as depicted in Figure 11, k_{11} of the mixed system was below the k_1 of the pure SDS solution; this suggested that the pure SDS solution made a greater contribution to the conductivity than the combination system at a common concentration of SDS. In terms of the HMBHAP/SDS mixed system, the small number of hydrophobic groups on the HMBHAPs molecular backbones formed mixed micelles with the SDS molecules through hydrophobic interactions. The k_{22} of the mixed system was practically similar to k_2; this showed that when the SDS concentration of the mixed system exceeded C_2, the contribution to the conductivity made by the mixed system was consistent with the pure SDS after cmc. This suggested that the combination of HMBHAPs with SDS was saturated, and normal surfactant micelles formed free in the system. As mentioned in the literature,[39,109] the mixed micelles formed by hydrophobically modified polymers with SDS have a higher degree of charge delocalization than those of a regular SDS micelle. Thus, the concentration corresponding to C_2 could be theoretically regarded as the cmc of SDS in the HMBHAP/SDS system, and the saturation binding capacity of the copolymers with SDS was located between C_1 and C_2.

On the other hand, k_{11} decreased with ascending N_H at the same concentrations of HMBHAPs. There was no doubt that the ionic strength of the mixed solutions decreased and made less contribution to the conductivity. So, the HMBHAPs with a longer microblock had more close-knit combinations with SDS; this led to the drop of the dissociation ability of the solutions and the ionic migration rate. This result also further confirmed the preceding interpretation for the viscosity measurements and fluorescence experiments. However, the reason why the increasing conductivity amplitude decreased and even leveled off was not demonstrated, and further discussion needs to be conducted in other works.

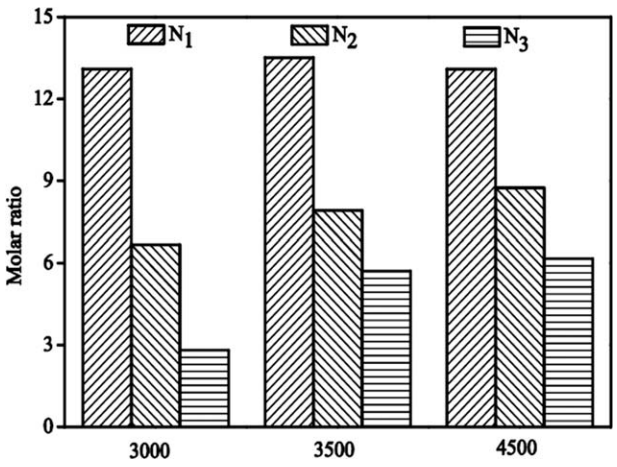

Figure 12. Binding molar ratios of SDS with the HMBHAPs at different copolymer concentrations (3000, 3500, and 4500 mg/L) as a function of the SDS concentration.

Binding Capacity of HMBHAPs with SDS

The previously obtained saturation binding capacity of SDS with HMBHAPs should have been between C_1 and C_2, but the value was not accurately calculated. Therefore, it could be acquired via the deduction of the cmc of the pure SDS from the cmc of SDS in the HMBHAP/SDS system. The results of the combination are shown in Table III and Figure 12. They show that the longer N_H was, the smaller the binding capacity was. This consequence could be interpreted as follows; the mixed micelle aggregation number in the solutions was composed of the hydrophobic side chains along the HMBHAPs backbones and the hydrophobic units of SDS. The aggregation number was fixed at a certain concentration of copolymers and SDS. When N_H was longer, the hydrophobic side chains contained in each block were much greater, and the hydrophobes of SDS required to saturate the mixed micelles were less. This demonstrated the interpretation for the lower SDS concentration corresponding to the I_3/I_1 platform with longer microblocks. The combination regimes were similar to the results reported in the literature,[56] where the binding capacity of the hydrophobically modified HEC with SDS at the maximum solution viscosity was 4:1 (the molar ratio of SDS and hydrophobes); this was obtained by the analysis of the combination viscosity, fluorescence, and NMR self-diffusion data. Last but not least, the binding capacity increased with the concentration of HMBHAPs when N_H was longer (N_2 and N_3). This phenomenon presented a consistent trend with the segment fitting slope k_{11} for the same HMBHAPs. So, this may have been due to the salt effect caused by the electrostatic interaction of carboxylate ions of copolymers, but this needs to be confirmed by other studies.

CONCLUSIONS

Hydrophobically associating poly(AM/NaAA/C_{12}AM)s with N_H's were prepared by micellar copolymerization, and the molecular structure was confirmed by FTIR spectroscopy, ^{1}H-NMR, and static light scattering. Then, the interaction strength and binding capacity of the copolymers with SDS were investigated by viscosity measurement, fluorescence, and conductometry. The results obtained by the viscosity measurement show that the viscosity of the mixed systems of the copolymers with SDS passed through a maximum (concentration of SDS $\approx 2 \times 10^{-3}$ mol/L) with increasing SDS concentration and reached a minimum at the cmc of SDS. More particularly, the increasing rates and amplitudes of viscosity increased with increasing N_H; on the contrary, the tackifying intervals decreased. From the fluorescence study, it was shown that in the pyrene emission spectra, the ratio of the third vibrational band to the first band (I_3/I_1) significantly increased with increasing SDS concentration and stabilized above a certain SDS concentration. The I_3/I_1 of different copolymer/SDS systems increased and stabilized at a lower SDS concentration with increasing N_H. In the conductivity experiments, all of the conductivity plots of the copolymer/SDS systems had two break points, and the conductivity increased nonlinearly between the inflection points. All of the results indicate that the interaction strength between the copolymers and SDS increased with N_H. Furthermore, we compared the cmc of SDS in the copolymer/SDS mixed systems with the cmc of the pure SDS solution, and the binding capacity was calculated from the difference. The results show that the binding capacity slightly decreased with increasing N_H. The conductometry needed to determine the binding capacity of SDS with copolymers was provided with a certain feasibility. However, the explanations for the nonlinear increase or platform of conductivity between break points C_1 and C_2 and the increase in binding capacity with increasing copolymer concentrations were not accurately given and needed to be discussed further.

ACKNOWLEDGMENTS

This work was supported by a grant from the National Science and Technology Major Project of China (contract grant number 2011ZX05011). The authors are grateful for the financial support.

REFERENCES

1. Ryles, R. *SPE Reservoir Eng.* **1988**, *3*, 23.
2. Sabhapondit, A.; Borthakur, A.; Haque, I. *Energy Fuels* **2003**, *17*, 683.
3. Stahl, G. A.; Schulz, D. Water-Soluble Polymers for Petroleum Recovery; Springer: New York, **1988**.
4. Lewandowska, K. *J. Appl. Polym. Sci.* **2007**, *103*, 2235.
5. Zhao, X.; Liu, L.; Wang, Y.; Dai, H.; Wang, D.; Cai, H. *Sep. Purif. Technol.* **2008**, *62*, 199.
6. Zhang, P.; Wang, Y.; Chen, W.; Yu, H.; Qi, Z.; Li, K. *J. Solution Chem.* **2011**, *40*, 447.
7. Nasr-El-Din, H.; Hawkins, B.; Green, K. In Proceedings of the 1991 SPE International Symposium on Oilfield Chemistry; Society of Petroleum Engineers: Dallas, TX, **1991**.
8. Sabhapondit, A.; Borthakur, A.; Haque, I. *J. Appl. Polym. Sci.* **2003**, *87*, 1869.
9. Guo, Y. J.; Liu, J. X.; Zhang, X. M.; Feng, R. S.; Li, H. B.; Zhang, J.; Lv, X.; Luo, P. Y. *Energy Fuels* **2012**, *26*, 2116.
10. Taylor, K. C. *Annu. Trans. Nord. Rheol. Soc.* **2003**, *11*, 13.
11. Pancharoen, M.; Thiele, M.; Kovscek, A. In Proceedings of the 2010 SPE Improved Oil Recovery Symposium; Society of Petroleum Engineers: Dallas, TX, **2010**.
12. Taylor, K. C.; Nasr-El-Din, H. A. *J. Pet. Sci. Eng.* **1998**, *19*, 265.
13. Buchgraber, M.; Clemens, T.; Castanier, L. M.; Kovscek, A. R. In Proceedings of the 2009 SPE Annual Technical Conference and Exhibition; Society of Petroleum Engineers: Dallas, TX, **1991**.
14. Dupuis, G.; Rousseau, D.; Tabary, R.; Grassl, B. *SPE J.* **2011**, *16*, 43.
15. Lu, H.; Feng, Y.; Huang, Z. *J. Appl. Polym. Sci.* **2008**, *110*, 1837.
16. Taylor, K.; Nasr-El-Din, H. In Proceedings of the 2007 SPE Canadian International Petroleum Conference; Society of Petroleum Engineers: Dallas, TX, **2007**; p 12.
17. Niu, Y.; Jian, O.; Zhu, Z.; Wang, G.; Sun, G. In Proceedings of the 2001 SPE International Symposium on Oilfield

Chemistry; Society of Petroleum Engineers: Dallas, TX, **2001**.

18. Feng, Y.; Billon, L.; Grassl, B.; Bastiat, G.; Borisov, O.; François, J. *Polymer* **2005**, *46*, 9283.
19. Feng, Y.; Billon, L.; Grassl, B.; Khoukh, A.; François, J. *Polymer* **2002**, *43*, 2055.
20. Randall, S. S. In Proceedings of the Oil & Natural Gas Technology Final Scientific/Technical Report; **2011**.
21. Wever, D.; Picchioni, F.; Broekhuis, A. *Prog. Polym. Sci.* **2011**, *36*, 1558.
22. Gouveia, L. M.; Paillet, S.; Khoukh, A.; Grassl, B.; Müller, A. *J. Colloids Surf. A* **2008**, *322*, 211.
23. Zhong, C.; Huang, R.; Xu, J. *J. Solution Chem.* **2008**, *37*, 1227.
24. Caputo, M. R.; Selb, J.; Candau, F. *Polymer* **2004**, *45*, 231.
25. Cram, S. L.; Brown, H. R.; Spinks, G. M.; Hourdet, D.; Creton, C. *Macromolecules* **2005**, *38*, 2981.
26. Kujawa, P.; Audibert-Hayet, A.; Selb, J.; Candau, F. *Macromolecules* **2006**, *39*, 384.
27. Noda, T.; Hashidzume, A.; Morishima, Y. *Langmuir* **2001**, *17*, 5984.
28. Noda, T.; Hashidzume, A.; Morishima, Y. *Macromolecules* **2001**, *34*, 1308.
29. Branham, K.; Davis, D.; Middleton, J.; McCormick, C. L. *Polymer* **1994**, *35*, 4429.
30. Smith, G. L.; McCormick, C. L. *Macromolecules* **2001**, *34*, 5579.
31. Smith, G. L.; McCormick, C. L. *Langmuir* **2001**, *17*, 1719.
32. Chassenieux, C.; Nicolai, T.; Benyahia, L. *Curr. Opin. Colloid Interface Sci.* **2011**, *16*, 18.
33. Feng, R.-S.; Guo, Y. J.; Zhang, X. M.; Hu, J.; Li, H. B. *J. Chem.* **2013**, *2013*, 6.
34. Goddard, E.; Hannan, R. *J. Am. Oil Chem. Soc.* **1977**, *54*, 561.
35. Moroi, Y.; Akisada, H.; Saito, M.; Matuura, R. *J. Colloid Interface Sci.* **1977**, *61*, 233.
36. Arai, H.; Murata, M.; Shinoda, K. *J. Colloid Interface Sci.* **1971**, *37*, 223.
37. Biggs, S.; Hill, A.; Selb, J.; Candau, F. *J. Phys. Chem.* **1992**, *96*, 1505.
38. Zana, R.; Kaplun, A.; Talmon, Y. *Langmuir* **1993**, *9*, 1948.
39. Biggs, S.; Selb, J.; Candau, F. *Langmuir* **1992**, *8*, 838.
40. Piculell, L.; Egermayer, M.; Sjöström, J. *Langmuir* **2003**, *19*, 3643.
41. Han, M.; Xiang, W.; Zhang, J.; Jiang, W.; Sun, F. In Proceedings of the 2006 International Oil & Gas Conference and Exhibition in China; Society of Petroleum Engineers: Dallas, TX, **2006**.
42. Zhou, W.; Zhang, J.; Han, M.; Xiang, W.; Feng, G.; Jiang, W. In Proceedings of the International Petroleum Technology Conference; Society of Petroleum Engineers: Dallas, TX, **2007**.
43. Xu, B.; Li, L.; Zhang, K.; Macdonald, P. M.; Winnik, M. A.; Jenkins, R.; Bassett, D.; Wolf, D.; Nuyken, O. *Langmuir* **1997**, *13*, 6896.
44. González Coronel, V.; Jiménez-Regalado, E. *Polym. Bull.* **2011**, *67*, 251.
45. English, R. J.; Laurer, J. H.; Spontak, R. J.; Khan, S. A. *Ind. Eng. Chem. Res.* **2002**, *41*, 6425.
46. Durand, A.; Hourdet, D. *Polymer* **1999**, *40*, 4941.
47. Feng, Y.; Grassl, B.; Billon, L.; Khoukh, A.; François, J. *Polym. Int.* **2002**, *51*, 939.
48. Jenkins, R. D.; Bassett, D. R. In Polymeric Dispersions: Principles and Applications; Asua, J. M., Ed.; NATO ASI Series*335*; Springer: New York, **1997**; p 477.
49. Dai, Z. Z. M.E. Thesis, Southwest Petroleum University, **2011**.
50. Jiménez-Regalado, E.; Selb, J.; Candau, F. *Langmuir* **2000**, *16*, 8611.
51. Annable, T.; Buscall, R.; Ettelaie, R.; Shepherd, P.; Whittlestone, D. *Langmuir* **1994**, *10*, 1060.
52. Bystryak, S. M.; Winnik, M. A.; Siddiqui, J. *Langmuir* **1999**, *15*, 3748.
53. Ghoreishi, S.; Fox, G.; Bloor, D.; Holzwarth, J.; Wyn-Jones, E. *Langmuir* **1999**, *15*, 5474.
54. Li, Y.; Ghoreishi, S.; Warr, J.; Bloor, D.; Holzwarth, J.; Wyn-Jones, E. *Langmuir* **1999**, *15*, 6326.
55. Li, Y.; Ghoreishi, S.; Warr, J.; Bloor, D.; Holzwarth, J.; Wyn-Jones, E. *Langmuir* **2000**, *16*, 3093.
56. Piculell, L.; Nilsson, S.; Sjostrom, J.; Thuresson, K. In Associative Polymers in Aqueous Media; Glass, J. E., Ed.; ACS Symposium Series*765*; American Chemical Society: Washington, DC, **2000**; Chapter 19, p 317.
57. Winnik, M. A.; Bystryak, S. M.; Chassenieux, C.; Strashko, V.; Macdonald, P. M.; Siddiqui, J. *Langmuir* **2000**, *16*, 4495.
58. Li, Y.; Xu, R.; Couderc, S.; Bloor, D.; Holzwarth, J.; Wyn-Jones, E. *Langmuir* **2001**, *17*, 5742.
59. Li, Y.; Xu, R.; Couderc, S.; Bloor, M.; Wyn-Jones, E.; Holzwarth, J. *Langmuir* **2001**, *17*, 183.
60. Li, Y.; Xu, R.; Couderc, S.; Ghoreishi, S.; Warr, J.; Bloor, D.; Holzwarth, J.; Wyn-Jones, E. *Langmuir* **2003**, *19*, 2026.
61. Sidhu, J.; Bloor, D.; Couderc-Azouani, S.; Penfold, J.; Holzwarth, J.; Wyn-Jones, E. *Langmuir* **2004**, *20*, 9320.
62. Couderc-Azouani, S.; Sidhu, J.; Thurn, T.; Xu, R.; Bloor, D.; Penfold, J.; Holzwarth, J.; Wyn-Jones, E. *Langmuir* **2005**, *21*, 10197.
63. Wang, H.; Wang, Y.; Yan, H.; Zhang, J.; Thomas, R. K. *Langmuir* **2006**, *22*, 1526.
64. Li, M.; Jiang, M.; Zhang, Y.; Fang, Q. *Macromolecules* **1997**, *30*, 470.
65. Panmai, S.; Prud'homme, R. K.; Peiffer, D. G.; Jockusch, S.; Turro, N. *J. Langmuir* **2002**, *18*, 3860.
66. Bromberg, L. E.; Barr, D. P. *Macromolecules* **1999**, *32*, 3649.
67. Mezei, A.; Mészáros, R. *Langmuir* **2006**, *22*, 7148.

68. Jansson, J.; Schillen, K.; Olofsson, G.; Cardoso da Silva, R.; Loh, W. *J. Phys. Chem. B* **2004**, *108*, 82.
69. Jones, M. N. *J. Colloid Interface Sci.* **1967**, *23*, 36.
70. Hou, Z.; Li, Z.; Wang, H. *J. Dispersion Sci. Technol.* **1999**, *20*, 1507.
71. Bataweel, M.; Nasr-El-Din, H. In Proceedings of the 2012 North Africa Technical Conference and Exhibition; **2012**.
72. Kamenka, N.; Burgaud, I.; Zana, R.; Lindman, B. *J. Phys. Chem.* **1994**, *98*, 6785.
73. Sovilj, V. J.; Petrović, L. B. *Carbohydr. Polym.* **2006**, *64*, 41.
74. Wang, Y. L.; Guo, Y. J.; Liu, J. X.; Feng, R. S. *Chin. J. Synth. Chem.* **2012**, *20*, 520.
75. Candau, F.; Volpert, E.; Lacik, I.; Selb, J. *Macromol. Symp.* **1996**, *111*, 85.
76. Volpert, E.; Selb, J.; Candau, F. *Macromolecules* **1996**, *29*, 1452.
77. Volpert, E.; Selb, J.; Candau, F. *Polymer* **1998**, *39*, 1025.
78. Candau, F.; Selb, J. *Adv. Colloid Interface Sci.* **1999**, *79*, 149.
79. Camail, M.; Margaillan, A.; Martin, I.; Papailhou, A.; Vernet, J. *Eur. Polym. J.* **2000**, *36*, 1853.
80. Candau, F.; Jimenez Regalado, E.; Selb, J. *Macromol. Symp.* **2000**, *150*, 241.
81. Grassl, B.; Francois, J.; Billon, L. *Polym. Int.* **2001**, *50*, 1162.
82. Kujawa, P.; Rosiak, J. M.; Selb, J.; Candau, F. *Macromol. Chem. Phys.* **2001**, *202*, 1384.
83. Vasiliadis, I.; Bokias, G.; Mylonas, Y.; Staikos, G. *Polymer* **2001**, *42*, 8911.
84. Kujawa, P.; Audibert-Hayet, A.; Selb, J.; Candau, F. *J. Polym. Sci. Part A: Polym. Chem.* **2003**, *41*, 3261.
85. Xue, W.; Hamley, I. W.; Castelletto, V.; Olmsted, P. D. *Eur. Polym. J.* **2004**, *40*, 47.
86. Lara-Ceniceros, A. C.; Rivera-Vallejo, C.; Jiménez-Regalado, E. *J. Polym. Bull.* **2007**, *58*, 425.
87. Biggs, S.; Selb, J.; Candau, F. *Polymer* **1993**, *34*, 580.
88. Hill, A.; Candau, F.; Selb, J. *Macromolecules* **1993**, *26*, 4521.
89. McCormick, C. L.; Nonaka, T.; Johnson, C. B. *Polymer* **1988**, *29*, 731.
90. Feng, R. S. D.E. Thesis, Southwest Petroleum University, **2008**.
91. Nilsson, S.; Thuresson, K.; Hansson, P.; Lindman, B. *J. Phys. Chem. B* **1998**, *102*, 7099.
92. Piculell, L.; Thuresson, K.; Lindman, B. *Polym. Adv. Technol.* **2001**, *12*, 44.
93. Mészáros, R.; Varga, I.; Gilányi, T. *Langmuir* **2004**, *20*, 5026.
94. Mészáros, R.; Varga, I.; Gilányi, T. *J. Phys. Chem. B* **2005**, *109*, 13538.
95. Zhou, W.; Dong, M.; Guo, Y.; Xiao, H. In 2003 Proceedings of the Canadian International Petroleum Conference; **2003**.
96. Zhou, W.; Dong, M.; Guo, Y.; Xiao, H. *J. Can. Pet. Technol.* **2004**, *43*, 13.
97. Zhao, D. M.E. Thesis, Southwest Petroleum University, **2010**.
98. Kujawa, P.; Audibert-Hayet, A.; Selb, J.; Candau, F. *J. Polym. Sci. Part B: Polym. Phys.* **2004**, *42*, 1640.
99. Kumacheva, E.; Rharbi, Y.; Winnik, M. A.; Guo, L.; Tam, K. C.; Jenkins, R. D. *Langmuir* **1997**, *13*, 182.
100. Horiuchi, K.; Rharbi, Y.; Spiro, J. G.; Yekta, A.; Winnik, M. A.; Jenkins, R. D.; Bassett, D. R. *Langmuir* **1999**, *15*, 1644.
101. Vorobyova, O.; Yekta, A.; Winnik, M. A.; Lau, W. *Macromolecules* **1998**, *31*, 8998.
102. Zhao, C. L.; Winnik, M. A.; Riess, G.; Croucher, M. D. *Langmuir* **1990**, *6*, 514.
103. Han, L. J.; Ye, Z. B.; Chen, H.; Luo, P. Y. *Acta Phys. Chim. Sin* **2012**, *28*, 1405.
104. Lan, J. H. M.E. Thesis, Dalian University of Technology, **2002**.
105. Dominguez, A.; Fernandez, A.; Gonzalez, N.; Iglesias, E.; Montenegro, L. *J. Chem. Educ.* **1997**, *74*, 1227.
106. Aguiar, J.; Carpena, P.; Molina-Bolıvar, J.; Carnero Ruiz, C. *J. Colloid Interface Sci.* **2003**, *258*, 116.
107. Fuguet, E.; Ràfols, C.; Rosés, M.; Bosch, E. *Anal. Chim. Acta* **2005**, *548*, 95.
108. Cai, L. *Univ. Chem.* **2003**, *18*, 54.
109. Zana, R.; Lianos, P.; Lang, J. *J. Phys. Chem.* **1985**, *89*, 41.